Composites Science and Technology 95 (2014) 38–43

Contents lists available at ScienceDirect

Composites Science and Technology

journal homepage: www.elsevier.com/locate/compscitech

AFM-based model of percolation in graphene-based polymer nanocomposites

Julia Syurik [a,*], Natalya Alyabyeva [b], Alexander Alekseev [c], Oleg A. Ageev [b]

[a] Institute of Microstructure Technology (IMT), Karlsruhe Institute of Technology (KIT), Hermann-von-Helmholtz-Platz 1, 76344 Eggenstein-Leopoldshafen, Germany
[b] Department of Micro- and Nanoelectronics, Southern Federal University (SFedU), Nekrasovsky, 44, Taganrog, Russia
[c] MCMP, School of Physics and Astronomy, Kelvin Nanocharacterization Centre, University of Glasgow, University Avenue, Glasgow G128QQ, United Kingdom

ARTICLE INFO

Article history:
Received 1 September 2013
Received in revised form 4 February 2014
Accepted 9 February 2014
Available online 19 February 2014

Keywords:
A. Nanocomposites
B. Electrical properties
C. Modeling
D. Scanning electron microscopy (SEM)
D. Atomic force microscopy (AFM)

ABSTRACT

Here, we show that a prediction of conductivity in composites can be improved by replacing fitting parameters of the percolation models by information on composite's microstructure. The methodology was demonstrated on the modified McCullough's structure-oriented model combined with current maps obtained by Conductive Atomic Force Microscopy (CA-AFM). The approach was tested on nanocomposites with graphene nanoplatelets (GNPs/PS) and proved to be coherent with experimental conductivity measurements and able to predict a percolation threshold. For the composite GNPs/PS both experimental and calculated percolation thresholds are approximately equal to 0.9 wt.% of GNPs. The model can be used for a prediction of conductivity of different kinds of conductive–dielectric composites.

1. Introduction

Polymer composites have been used industrially for over 110 years [1]. The discovery of graphene [2,3], a light, stiff material with the unique conductive properties, gave a rise to a novel class of materials – polymer nanocomposites with graphene [4,5]. Graphene nanoplatelets (GNPs) are thin nanodisks with high aspect ratio consisting of up to 10 graphene monolayers stacked together [6,7]. The morphology of nanoplatelets allows the platelets to provide barrier properties efficiently, while their pure graphitic composition makes them excellent electrical and thermal conductors. Such composites have a tunable conductivity level in the range of 10^{-11}–10^{2} S/m and, as a result, can find different applications, for example as antistatic coatings [5,8,9].

At a certain loading of graphene the electrical conductivity of nanocomposites with graphene nanoplatelets (GNPs-NC) drastically grows up to thirteen orders of magnitude. This loading is called a percolation threshold, graphene in this case is a filler and a polymer is a matrix [10–12]. The percolation threshold is an indicator of quality and fine functionality of a composite. It should be as low as possible in order to reduce the use of graphene and reproducible in order to obtain the composite with a desired functionality. Nowadays, the lowest percolation thresholds for GNPs-NC are less than 0.5 wt.% and reach 0.1 wt.% [13]. The most important parameters influencing the percolation threshold are dispersion, a shape of the filler, physicochemical interactions between the matrix and the filler and a method used to obtain the composite. As there are so many parameters, the prediction of the conductive properties is critical.

Various models were proposed to predict the conductive behavior of composites. These models consider different assumptions and can be classified as statistical [10,14,15], thermodynamic [16–18] and structure-oriented [19]. The most conforming class of models is structure-oriented [19]. These models consider a microstructure of nanocomposites before or after the final processing. However, at the time they were developed the methods allowing realistic description of the composite's microstructure did not exist. Therefore, in the models mentioned above the composite's microstructure is replaced by fitting parameters.

Atomic force microscopy (AFM) became a powerful tool of investigation the morphology and electro physical properties of nanocomposites. In this study we propose a method allowing replacement the empirical fitting parameters by the information about the real morphology of the composite obtained with AFM. The method is demonstrated on the McCullough's structure oriented model [19].

2. The McCullough's model

In the McCullough's model [19] a microstructure of the composite and an orientation of the filler particles inside the composite are

* Corresponding author. Tel.: +49 72160820462; fax: +49 72160824331.
E-mail address: julia.syurik@kit.edu (J. Syurik).

http://dx.doi.org/10.1016/j.compscitech.2014.02.006
0266-3538/

assumed to change with the concentration. Below the percolation threshold the filler particles aggregate in chains. The aspect ratio of the chains depends on a shape and a concentration of the filler in the composite. It is assumed that after the percolation threshold all smaller chains are connected in a conducting network. The formation of the chains is statistical in nature. Therefore, a distribution of chains' lengths will occur. The distribution can be described by a probability density function $n(v_f, a)$ resulting in a distribution of an effective aspect ratio a for a specified volume fraction v_f of the filler. Thus, the average value of the chain parameter $\langle\lambda\rangle$ is given by [19]:

$$\langle\lambda\rangle = \int_1^\infty n(v_f, a)\lambda(a)da, \tag{1}$$

where $\int_1^\infty n(v_f, a)\lambda(a)da = 1$ and $\lambda(a)$ is a chain parameter, depending on a filler shape. For the filler particles with an aspect ratio a exceeding 1, the chain parameter can be found as [19]:

$$\lambda(a) = 1 - A^2\left(1 - 0.5\left(A - A^{-1}\right)\ln\left(\frac{A+1}{A-1}\right)\right), \tag{2}$$

where $A^2 = \frac{a}{1-a^2}$.

The distribution $n(v_f, a)$, and hence $\langle\lambda\rangle$, is a function of concentration v_f. The final equation for the isotropic distribution of the filler particles appears as [19]:

$$\frac{\sigma_m}{\sigma} = \frac{v_m^2(1-\langle\lambda\rangle)}{V_m} + \frac{\sigma_m}{\sigma_f}\cdot v_f \cdot \frac{V_m^2 + v_m(1+V_m)\langle\lambda\rangle}{V_m^2}, \tag{3}$$

where $\frac{\sigma_m}{\sigma_f} << 1, \quad V_m = (1-\langle\lambda\rangle)v_m + \langle\lambda\rangle v_f$,

σ_m, σ_f, σ-electrical conductivities of the matrix, the filler and the composite respectively; v_f, v_m-volume fractions of the filler and the matrix. The complete characterization of $n(v_f, a)$ and the subsequent evaluation for $\langle\lambda\rangle$ is a tedious experimental task. However, λ and its average $\langle\lambda\rangle$ might be chosen as fitting parameters through the assumed aspect chain ratio a. An avoiding real microstructure of the composite brings a limitation to the model and a semi-empirical character of the Eq. (3). We have developed the technique of extracting the value for $\langle\lambda\rangle$ from the AFM-obtained data on composite's microstructure. The technique is demonstrated for the composite with polystyrene and graphene nanoplatelets (GNPs/PS).

3. A modification of the percolation model

A calculation of the chain parameter $\langle\lambda\rangle$ for ideal filler shapes (spheres, disks, ropes) according to the equations proposed in [19] allows to substitute $\langle\lambda\rangle$ by:

$$\langle\lambda\rangle \cong \lambda(\langle\grave{a}^2\rangle), \tag{4}$$

where $\langle\grave{a}^2\rangle$ – a mean-square value of the aspect ratio a of the conductive chain.

If the data on two-dimensional chain distribution is obtained (as it is possible with AFM in CA-AFM mode) the value of $\langle\grave{a}^2\rangle$ may be found as:

$$\langle\grave{a}^2\rangle = \frac{1}{n}\sum_{i=1}^{n}\left(\frac{l_i}{d_i}\right)^2 = \left(\frac{\langle l\rangle}{\langle d\rangle}\right)^2 \tag{5}$$

where n – the number of conductive chains; l_i – the length of the ith chain; d_i – the diameter of the ith chain; $\langle l\rangle$ and $\langle d\rangle$ – the average length and diameter of the chain.

The evaluation of the right part of the Eq. (3) for the GNPs/PS composite shows that due to the low electrical conductivity of the matrix (10^{-9} S/m) and high conductivity of the filler (10^4 S/m), the first term is 5–7 orders of magnitude larger. Therefore, the Eq. (3) for the chosen type of nanocomposite can be reduced to:

$$\frac{\sigma_m}{\sigma} = \frac{v_m^2(1-\langle\lambda\rangle)}{V_m}, \tag{6}$$

where $\langle\lambda\rangle$ is described by Eqs. (4) and (5).

The density of the composite can be found as a sum of densities of the filler and the matrix taken according to their volume fractions:

$$\rho = \rho_f v_f + \rho_m(1-v_f), \tag{7}$$

where ρ – specific density of the composite, kg/m^3; ρ_f – specific density of the filler, kg/m^3; ρ_m – specific density of the matrix, kg/m^3.

When one uses GNPs as a filler, the resulting composite contains micro- and nanopores, influencing the bulk conductivity of the composite. We propose to consider the pores by using an apparent density ρ_{ap} connected with the specific density through the pores coefficient:

$$K_p = \rho_f/\rho_{ap}. \tag{8}$$

Assuming that the composites are produced by a reproducible technology (i.e. latex technology [20]) the K_p can be calculated only once from the measured properties of the produced nanocomposite and used for the conductivity prediction afterwards.

Then, Eq. (7) can be transformed to:

$$\rho = \rho_f v_f/K_p + \rho_m(1-v_f). \tag{9}$$

The coefficient K_p depends on geometry of the filler and on the technology of the composite's production. The value of ρ_{ap} can be defined experimentally if the sample's mass m, the volume V and the filler loading w are known

$$\frac{\rho_f}{K_p} = \frac{m\cdot w}{V - \frac{m(1-w)}{\rho_m}}. \tag{10}$$

From the Eq. (7) the volume fraction of the filler can be calculated as:

$$v_f = \frac{\rho - \rho_m}{\frac{\rho_f}{K_p} - \rho_m}. \tag{11}$$

Usually the loading of the filler in composites is expressed as a weight fraction (wt.%), therefore it is useful to change the volume fractions to weight fractions:

$$G = v_f/w_f, \tag{12}$$

where G – can be calculated by combining Eqs. (11) and (12).

$$\frac{\sigma_m}{\sigma} = \frac{G^2(1-w_f)^2(1-\langle\lambda\rangle)}{V_m}, \tag{13}$$

$$V_m = (1-\langle\lambda\rangle)G(1-w_f) + \langle\lambda\rangle G w_f, \tag{14}$$

the Eqs. (13) and (14) describe a conductivity behavior vs. filler loading. To solve these equations such known material properties and experimental parameters as the weight fraction of the filler w_f the mass of the sample m, the pores coefficient K_p, the specific density of the filler ρ_f, and the specific density of the matrix ρ_m should be used in a combination with the average chain parameter $\langle\lambda\rangle$.

4. AFM-based technique of $\langle\lambda\rangle$ evaluation

In order to obtain a value of $\langle\grave{a}^2\rangle$ and $\langle\lambda\rangle$ a technique based on analysis of an AFM-image obtained in the CA-AFM mode [23] was developed. A standard CA-AFM image should be imported to a software allowing for a statistical analysis. In the current experiment the scanning was performed with a probe station Ntegra Vita (NT-MDT, Russia) which goes together with Image Analysis

2.0 software. As the CA-AFM method gives a current distribution, one can interpret the clusters with a similar non-zero current level as separate graphene clusters incorporated into the dielectric matrix with a near-zero current. One should set a threshold of a minimum current level which will be associated with graphene clusters. The CA-AFM image of the GNPs/PS composite is presented in Fig. 1a. The corresponding image of the grains is shown in Fig. 1b where 368 grains are demonstrated. The histogram (Fig. 1c) presents a size distribution of the GNP clusters. For each graphene cluster the information on the grain aspect ratio, the number, the average length and the diameter is available for the analysis. Based on the statistical data the calculations of $\langle \grave{a}^2 \rangle$ (Eq. (6)) and $\langle \lambda \rangle$ (Eq. (4)) can be done for all samples of nanocomposites and used for the conductivity calculations afterwards.

5. Sample preparation

Samples of composites with polystyrene and graphene nanoplatelets (GNPs/PS) were prepared by latex technology being the only technology allowing the reproducible percolation threshold [20]. The preparation procedure is described in details in [22]. According to the AFM analysis after sonication, the most of the GNPs have a thickness corresponding to 2–3 atomic layers, the average surface area of the GNPs ranged from 1 to 3 μm^2. The obtained dispersion was mixed with PS latex in sufficient concentration followed by a compression moulding. Nanocomposite samples were produced with various loadings of GNPs (0, 0.6, 0.9, 1.5, 2.0 wt.%).

6. Characterization of the nanocomposites

6.1. Scanning electron microscopy (SEM)

The morphology of composites was characterized with a FEI Nova Nanolab 200 (Fei Co.) equipped with a field emission electron source. A secondary electron detector was used for image acquisition in high vacuum conditions. No additional sample treatment has been performed. Standard acquisition conditions for a charge contrast imaging were applied [21].

6.2. Micro scale characterization: CA-AFM measurement

Quantitatively the morphology and electrical properties of the composite's surface investigated with the probe station Ntegra Vita (NT-MDT, Russia) operated in CA-AFM mode allowing mapping the conductive properties of the surface with a resolution of a few nanometers [23]. Freshly prepared surfaces obtained by nitrogen freezing and cutting were investigated. The cantilevers NSG11 (NT-MDT) with a conductive W_2C coating were used (tip radius 35 nm). The measurements were performed on air at 23 °C, and 45% humidity. The scan size was 5 × 5 μm. For each sample the obtained topological parameters, i.e. the average length and diameter of the chain, represent the average length or diameter of all clusters detected in the scan. Such an assumption was taken due to the reproducibility of the latex technology and a relatively big scan area.

6.3. Macro measurements of electrical conductivity

Macro electrical conductivity measurements in DC mode were performed in a direction parallel to the sample top surface using a 2-probe configuration and a Keithley 2602 system source meter. Conductivity was calculated from the obtained I/V characteristics according to the following equation:

$$\sigma = \frac{b \cdot I}{V \cdot A}, \tag{15}$$

where V – an applied voltage, I – a measured current through a cross-section A between the distance b. The used values for b and A are shown in Table 2.

The conductivity was measured between the two gold electrodes with dimensions of 1 × 4 mm^2 and a thickness of around 100 nm. The samples had sizes of 5 × 9 mm^2 and varying thickness between 45 μm and 560 μm. All contacts showed linearity of the $I(V)$ dependency and thus are ohmic. For each sample the

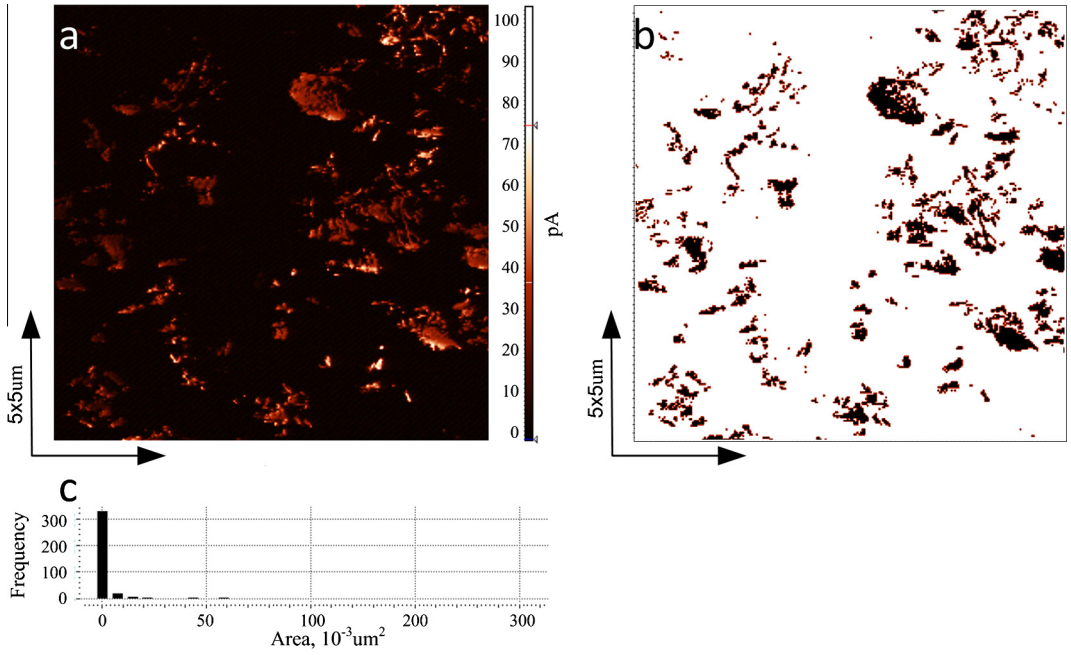

Fig. 1. An overview of the process of cluster analysing: (a) CA-AFM image of the GNPs/PS composite, the scan size in 5 × 5 μm; (b) the corresponding image of the grains; (c) the histogram presenting a size distribution of the GNP clusters.

conductivity data represent the average value of 10 consecutive measurements.

7. Results and discussion

7.1. Scanning electron microscopy analysis

The charge contrast imaging SEM mode is applicable to the composites above the percolation threshold, where the conductive network of GNPs is formed inside the dielectric matrix. High accelerating voltages with incident beam energy of 20 keV were used for imaging of as-produced nanocomposites. For such imaging conditions graphene nanoplatelets appear bright against dark polymer matrix. The nature of such contrast can be explained by a difference in the amount of secondary electrons generated in GNPs and polystyrene. The detailed discussion of the contrast can be found in [8,21].

The charge contrast images of GNPs/PS composites with various GNP loadings are demonstrated in Fig. 2a–d. For the low GNS loadings the sample is charged and the image mainly shows artefacts (Fig. 2 a). For the higher a bright contrast of GNPs appears in the dark polymer matrix. The contrast is stronger for the samples with higher GNP loading as such samples have an increased value of primary electrons (PEs) which dissipate through the GNPs neutralizing the negative charge of the dielectric matrix. Brighter GNP regions are believed to be located closer to the sample surface, while greyish ones are located deeper into the volume [21]. For all cases GNPs are bended and even folded (the best can be identified in Fig. 2 d). The GNP sheets have sizes of a few micrometers and are randomly oriented. However, due to the GNP shape and the contrast mechanism the eye catches mainly platelets oriented perpendicular to the PE beam which is parallel to the sample top surface.

7.2. Atomic force microscopy images analysis

The CA-AFM images (Fig. 2e–h) of the composites' surface are presented. The corresponding morphology images do not contain information about GNP distribution and, therefore, are not shown According to the CA-AFM imaging, for the sample with 0.6 wt.% of GNPs the average diameter is roughly twice as big as other samples (Table 1). For the samples with higher GNPs loadings the average diameter of the chain does not depend on the GNP loading. One could suggest that the used technique allows imaging only a small part of the GNP network lying close to the scanned surface [24].

Similar to the SEM images (Fig. 2a–d) the CA-AFM images (Fig. 2e–h) contain volume information about the composite. For SEM method the imaging depth depends on the accelerating voltage [21], for the CA-AFM – on the applied potential [23]. GNPs appear in clusters, which can be considered as conductive chains embedded in the matrix. The number of such chains is increasing with GNP loading (Table 1), alongside with the 5.7 times increasing of the average chain length.

Thus, for the sample with 2 wt.% of GNPs the average chain length is 3 times more than the average size of a single graphene nanoplatelets taken from AFM analysis of just produced GNPs [22]. However, it should be taken into account that in the composites the GNPs are randomly distributed being folded and bended (Fig. 2b–d). Therefore, the conductive chains in GNPs/PS composites should consist of bigger amount of GNPs.

The conductivity dependence on GNP loading (Fig. 3, curve 1) is well-known for this class of composites [8,14]. For the low GNP loadings the conductivity of the GNPs/PS is close to the conductivity of the PS matrix. The percolation threshold is equal to 0.9 wt.% of GNPs. At this GNP loading the conductivity is increasing by 5 orders of magnitude and reaches 8 S/m for the sample with 2 wt.% of GNPs.

Based on the presented methodic the average length $\langle l \rangle$ and diameter $\langle d \rangle$ of the conductive GNPs clusters have been obtained (Table 1) and used in order to calculate the mean-square value of an aspect ratio $\langle \grave{a}^2 \rangle$ (Eq. (5), Table 1). In presented composites the aspect ratio increases in 8.7 times with an increase of GNP loading. Thus, the uncertainty of the mean-square deviation $\sqrt{\langle \grave{a}^2 \rangle}$ decreases with GNP loading. The values of $\langle \lambda \rangle$ for all composites (Table 1) are in the range $0 < \langle \lambda \rangle < 1$ and therefore lie in the restrictions of the McCullough's model [19]. The dependence of $\langle \lambda \rangle$ on $\sqrt{\langle \grave{a}^2 \rangle}$ is presented (Fig. 4). For the sample with 0.9 wt.% GNP loading the mean-square deviation $\sqrt{\langle \grave{a}^2 \rangle} = 5.3$ and $\langle \lambda \rangle = 0.919$. The latter tends asymptotically to 1 with an increase of GNP loading. Therefore, the GNP loading of 0.9 wt.% can be interpreted as the percolation threshold being in agreement with the results of CA-AFM measurements.

The calculations of the conductivity of the GNPs/PS nanocomposites were performed by Eqs. (10)–(14) with coefficients presented in Table 2. The resulting conductivity vs. GNP loading plot is shown in Fig. 3 (curve 4) and Table 1. In order to estimate the

Table 2
The parameters for conductivity calculation.

Parameter		Value
Density of polystyrene, kg/m^3		1060 [25]
Density of graphite, kg/m^3		1300 [26]
GNP loading, wt.%		0.6; 0.9; 1.5; 2.0
Sample's mass (0.9 wt.% GNP loading), kg		$0.017 \cdot 10^{-3}$
Sample's dimensions, m, and volume, m^3 (taken at 0.9 wt.% GNP loading)	a	$4.4 \cdot 10^{-4}$
	b	$8 \cdot 10^{-3}$
	c	$5.5 \cdot 10^{-3}$
	V	$1.936 \cdot 10^{-8}$
K_p		0.027
v_f		0.18
G		17.99

Table 1
The chain parameter and conductivity of GNPs/PS nanocomposite.

Parameter		Number/name of samples			
GNP loading, wt.%		0.6	0.9	1.5	2
The grain number, n		203	226	334	387
$\langle l \rangle$, nm		98 ± 10	118 ± 19	247 ± 28	561 ± 37
$\langle d \rangle$, nm		49 ± 4	22 ± 4	24 ± 4	32 ± 4
$\sqrt{< a^2 >}$		2.0 ± 0.3	5.3 ± 0.5	10.1 ± 0.9	17.3 ± 0.9
$\langle \grave{a}^2 \rangle$		4.0 ± 0.3	28.9 ± 0.5	102.02 ± 0.9	299.29 ± 0.9
$\langle \lambda \rangle$	Calculated	0.768	0.919	0.967	0.985
	Calculated based on [19]	$\langle \lambda \rangle \to 0.67$	–	–	$\langle \lambda \rangle \to 1 (\approx 0.99999)$
σ, S/m	Calculated	$(1.05 \pm 0.08) \cdot 10^{-9}$	$(1.10 \pm 0.1) \cdot 10^{-4}$	0.14 ± 0.01	3.04 ± 0.01
	Calculated based on [19]	$(1.39 \pm 0.09) \cdot 10^{-9}$	–	–	0.08 ± 0.01
	CA-AFM	$(8.0 \pm 0.5) \cdot 10^{-8}$	$(1.1 \pm 0.1) \cdot 10^{-4}$	0.30 ± 0.02	8.0 ± 0.1
	DC	$<2.35 \cdot 10^{-9}$	$(2.18 \pm 0.06) \cdot 10^{-4}$	1.78 ± 0.05	11.92 ± 0.08

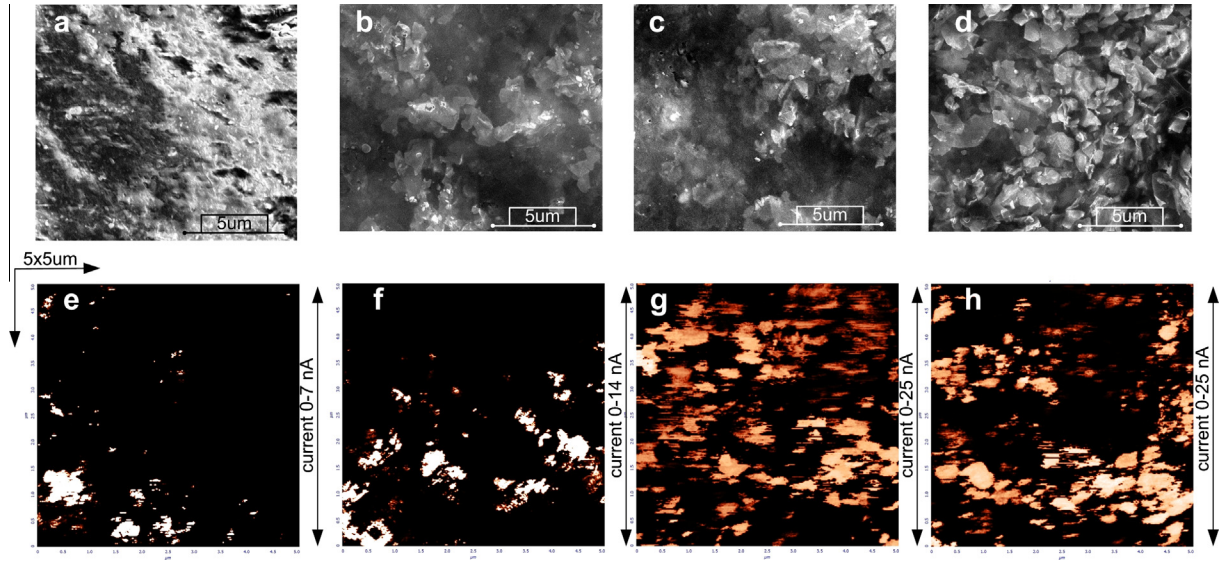

Fig. 2. Characterization of the GNPs/PS composites with different GNP loadings: (a–d) SEM charge contrast images with a scale bar of 5 μm; (e–h) CA-AFM images. Scan size is 5 × 5 μm. The GNP loadings are 0.6, 0.9, 2.0 and 1.5 wt.% for the 1st, 2nd, 3rd and 4th columns respectively.

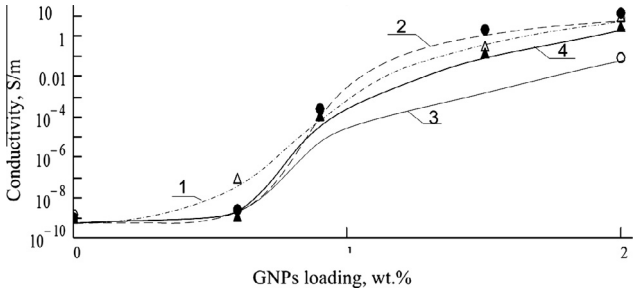

Fig. 3. The experimentally obtained dependencies of the conductivity of the GNPs/PS nanocomposite via GNP loading obtained via CA-AFM (curve 1) and macro conductivity measurements (curve 2) and a comparison with the McCullough's model (curve 3) and the developed model (curve 4).

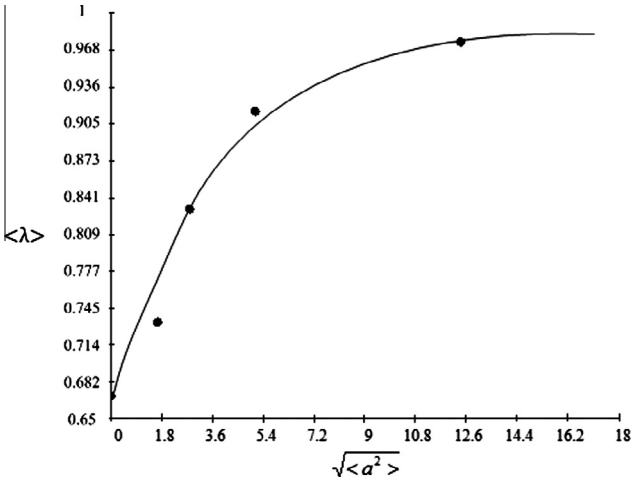

Fig. 4. The dependence of the average chain parameter on the mean-square value of the aspect ratio.

accuracy of the developed model the conductivity curve based on McCullough's model is also plotted (Fig. 3, curve 3). The comparison of these two models with experimental DC macro measurements of conductivity of the GNPs/PS composite is shown in the following section.

7.3. Electrical conductivity analysis

The conductivity dependence on the GNP loading for the GNPs/PS composites (Table 3 and Fig. 3, curve 2) measured by 2-point DC measurements is similar to one measured by CA-AFM (Fig. 3, curve 1). At low GNP loadings the conductivity of the GNPs/PS composites is very close to the conductivity of the dielectric polymer matrix, because no conductive GNP network is formed.

According to the DC measurements the composite exhibits the conductivity percolation threshold at GNP loading of around 0.9 wt.% being in agreement with the data from SEM and CA-AFM. The curve obtained by DC measurements shows a sharp percolation threshold. At this concentration the composite's conductivity increases drastically by 5 orders of magnitude. The conductivity of the sample before percolation threshold (Table 1, sample with 0.6 wt.% of GNPs) obtained with CA-AFM is one order of conductivity higher, than for DC data. This might be explained by a presence of microscopic conductive subnetworks of GNPs [8] (Table 1) influencing local CA-AFM measurements. However, these subnetworks are do not create the full network. Thus, there is no a conductive pathway between two macro electrodes during DC measurements and the macroscopic conductivity of such composite has the level of insulating matrix. For the samples after percolation threshold, where the conductive pathway is created, (Table 1, sample with 0.9 wt.% of GNPs) the conductivity obtained by DC measurements and CA_AFM has the same order of magnitude. At the GNP loading of about 2 wt.%, the conductivity level reaches 12 S/m.

8. Conclusion

We have improved the McCullough's model for predicting the electrical conductivity of conductive composites by replacing fitting parameters of the model by the data on composite's microstructure. The proposed model was tested on graphene-based nanocomposites and proved to be coherent with the experimental conductivity measurements. Moreover, both experimental and modeled data are described by a similar value of the percolation

Table 3
The cross-section, taken current path, as measured I/V data sets and corresponding conductivities of the composite samples. Relative error is about 10%.

Parameter	GNPs /PS (GNP loading, wt.%)			
	0.6	0.9	1.5	2
b, mm	5	5	5	5
A, mm^2	0.62	0.36	0.18	0.68
S conductance, S (as measured)	$<3.00 \cdot 10^{-11}$	$1.57 \cdot 10^{-8}$	$6.43 \cdot 10^{-7}$	$5.41 \cdot 10^{-5}$
Conductivity σ, S/m (calculated)	$<2.35 \cdot 10^{-9}$	$2.18 \cdot 10^{-4}$	1.78	11.92

threshold. A comparison with the conductivity prediction based on the McCullough's model shows that the conductivity value for the sample with 0.6 wt.% loading of GNPs is within the accuracy. However, for the sample with 2.0 wt.% of GNPs the conductivity of the sample is about one order of magnitude lower than the experimentally obtained value. Considering the overall conductivity difference of 10 orders of magnitude for the composites with different GNPs loadings, a mismatching between predicted and experimentally measured conductivity is relatively small.

To conclude, the proposed model basing on the composite's microstructure describes the experimental data more accurate than the prototype one. The model can be used for the prediction of conductivity of different kinds of conductive–dielectric composites.

Acknowledgements

We are indebted to Evgeniy Tkalya and Marcos Ghislandi (Technical University of Eindhoven) for providing the samples. The present work benefited from the input of Prof. Dr. Joachim Loos (DSM Resolve) who helped with improving of the manuscript.

This work was financially supported by the Program of development of Southern Federal University.

References

[1] Bledzki AK, Gassan J. Composites reinforced with cellulose based fibers. Prog Polym Sci 1999;24(2):221–74.
[2] Geim AK, Novoselov KS. The rise of graphene. Nat Mater 2007;6(3):183–91.
[3] Park S, Ruoff RS. Chemical methods for the production of graphenes. Nat Nanotechnol 2009;4(4):217–24.
[4] Stankovich S, Dikin DA, Dommett GH, Kohlhaas KM, Zimney EJ, Stach EA, et al. Graphene-based composite materials. Nature 2006;442(7100):282–6.
[5] Huang X, Qi X, Boey F, Zhang H. Graphene-based composites. Chem Soc Rev 2012;41(2). 666–6.
[6] Shao Y, Zhang S, Wang C, Nie Z, Liu J, Wang Y, et al. Highly durable graphene nanoplatelets supported Pt nanocatalysts for oxygen reduction. J Power Sources 2010;195(15):4600–5.
[7] Shen J, Hu Y, Li C, Qin C, Shi M, Ye M. Layer-by-layer self-assembly of graphene nanoplatelets. Langmuir 2009;25(11):6122–8.
[8] Syurik YV, Ghislandi MG, et al. Graphene network organisation in conductive polymer composites. Macromol Chem Phys 2012;213(12):1251–8.
[9] Kuilla T, Bhadra S, Yao D, Kim NH, Bose S, Lee JH. Recent advances in graphene based polymer composites. Prog Polym Sci 2010;35(11):1350–75.
[10] Stauffer D, Aharnoy A. Introduction to percolation theory. London: Taylor and Francis; 1991. p. 304.
[11] Martin CA, Sandler JKW, Shaffer MSP, Schwarz MK, Bauhofer W, Schulte K, et al. Formation of percolating networks in multi-wall carbon-nanotube–epoxy composites. Compos Sci Technol 2004;64(15):2309–16.
[12] Grunlan JC, Mehrabi AR, Bannon MV, Bahr JL. Water-based single walled nanotube filled polymer composite with an exceptionally low percolation threshold. Adv Mater 2004;16(2):150–3.
[13] Eda G, Chhowalla M. Graphene-based composite thin films for electronics. Nano Lett 2009;9(2):814–8.
[14] Zallen R. The physics of amorphous solids. New York: Wiley; 1983 [Chapter 4].
[15] Kirkpatrick S. Percolation and conduction. Rev Mod Phys 1973;45:574.
[16] Sumita M, Sakata K, Asai S, Miyasaka K, Nakagawa H. Effects of organic dispersants on the dispersion, packing, and sintering of alumina. Polym Bull 1991;25:265.
[17] Sumita M, Asai A, Miyadera N, Jojima E, Miyasaka K. Electrical conductivity of carbon black filled ethylene-vinyl acetate copolymer as a function of vinyl acetate content. Colloid Polym Sci 1986;264:212–7.
[18] Miyasaka K et al. Electrical conductivity of carbon–polymer composites as a function of carbon content. J Mater Sci 1982;17(6):1610–6.
[19] McCullough RL. Generalized combining rules for predicting transport properties of composite materials. Compos Sci Technol 1985;22:3–21.
[20] Berger MA, McCullough RL. Characterization and analysis of the electrical properties of a metal-filled polymer. Compos Sci Technol 1985;22:81–106.
[21] Loos J, Alexeev A, Grossiord N, Koning CE, Regev O. Visualization of single-wall carbon nanotube (SWNT) networks in conductive polystyrene nanocomposites by charge contrast imaging. Ultramicroscopy 2005;104(2):160–7.
[22] Tkalya E et al. Latex-based concept for the preparation of graphene-based polymer nanocomposites. J Mater Chem 2010;20(15):3035–9.
[23] Eyben P et al. Scanning spreading resistance microscopy and spectroscopy for routine and quantitative two-dimensional carrier profiling. J Vac Sci Tech B: Microelectron Nanometer Struct 2002;20(1):471–8.
[24] Alekseev A et al. Three-dimensional electrical property mapping with nanometer resolution. Adv Mater 2009;21:1–5.
[25] Watson WD, Wallace TC. Polystyrene and styrene copolymers. Applied polymer science. ACS Symposium Series, 1985. p. 285.
[26] Novoselov KS et al. Electronic properties of graphene. Phys Status Solidi (B) 2007;244(11). 4106–1.